



## Temperature Variation with Hemodynamic Effect Simulation on Wall Shear Stress in Fusiform Cerebral Aneurysm

Ahmad Faiz Mat Zin<sup>1,\*</sup>, Ishkriyat Taib<sup>2</sup>, Muhammad Hanafi Asril Rajo Mantari<sup>1</sup>, Bukhari Manshoor<sup>2</sup>, Ahmad Mubarak Tajul Arifin<sup>2</sup>, Mahmud Abd Hakim Mohamad<sup>1</sup>, Muhammad Sufi Roslan<sup>1</sup>, Muhammad Rafiuddin Azman<sup>2</sup>

<sup>1</sup> Product Research and Development Group, Centre for Diploma Studies, Universiti Tun Hussein Onn Malaysia, Pagoh Education Hub, 84600 Pagoh, Johor, Malaysia

<sup>2</sup> Department of Mechanical Engineering, Faculty of Mechanical Engineering and Manufacturing, Universiti Tun Hussein Onn Malaysia, 86400 Batu Pahat, Johor, Malaysia

### ARTICLE INFO

#### Article history:

Received 29 January 2022

Received in revised form 15 April 2022

Accepted 20 April 2022

Available online 22 May 2022

#### Keywords:

Aneurysm; middle cerebral artery; fusiform; wall shear stress; hypertension

### ABSTRACT

A cerebral aneurysm is the dilation of an arterial wall and mostly occurs at the weak point in the arterial circulation in the brain. Approximately 85% of aneurysms are in the anterior circulation, predominately at junctions, or bifurcations along the circle of Willis. Several studies have been conducted by researchers to analyse the blood flow characteristic and flow on the aneurysmal wall, however, there are small numbers of research focus on the fusiform aneurysm and the effect of temperature on the blood flow inside the aneurysm. Thus, this study aims to analyse the body temperature effect on hemodynamic parameters in the fusiform aneurysm. Three different models of the fusiform aneurysm based on patient-specific geometries have been developed and simulated. The computational Fluid Dynamics (CFD) method was imposed in this study to analyse the effect of hemodynamic variables on the different body temperatures by analysing the Wall Shear Stress (WSS) and Oscillatory Shear Index (OSI) at the fusiform aneurysmal wall. The result shows that the WSS values fluctuate with the temperature variations and were observed lowest low at the anterior fusiform aneurysm. The OSI indicates similar results for each physiological condition with the variation of temperature. The high value of WSS and low value of OSI increase the possibility of an aneurysmal wall being ruptured.

## 1. Introduction

Cerebral aneurysms are a major contributor to the rising number of deaths caused by severe haemorrhages caused by their rupture. Because hemodynamic influence and body temperature contribute significantly to the progression and formation of cerebral aneurysms, it is critical to investigate how these parameters can increase the aneurysm's chances of growth and rupture. Because fusiform type cerebral aneurysms are rare and hard to treat, few measures are taken to manage this type of aneurysm [1,2]. However, if not properly treated, this type of aneurysm can be

\* Corresponding author.

E-mail address: [ahmadfaiz@uthm.edu.my](mailto:ahmadfaiz@uthm.edu.my)

<https://doi.org/10.37934/arfmts.95.2.4054>

a factor contributing to severe haemorrhage. The number of cases is growing, and they are associated with a higher re-bleeding rate and mortality [3,4].

In their study, Miao Li *et al.*, [5] simulate 16 intracranial aneurysms. At the aneurysm sac and rupture point, hemodynamic parameters, WSS, and OSI were calculated. They discovered that the value of WSS was significantly higher at the aneurysm sac than at the rupture point. According to Jiang *et al.*, [6], higher pressure and lower WSS are associated with thinning of the local aneurysm wall. Based on unruptured actual medical cases, they simulated a saccular aneurysm with a thin-walled region and a relatively normal thickness area in the study. In their simulation, Jiang *et al.*, [7] imposed three different cardiac frequencies to the patient-specific geometry of the cerebral aneurysm. With an increase in heart rate, the flow pattern and WSS change significantly. Isaksen *et al.*, [8] investigated the location of high wall tension area and displacement in the aneurysm wall using a patient-specific model in their computational fluid dynamic simulation of saccular cerebral aneurysm. They claim that the typical location of rupture is at a point of high wall tension and is dependent on the shape of the aneurysm. In their work, Xu *et al.*, [9] suggest that fluctuations in the values and frequency of WSS contributed to the rupture of the aneurysm in terms of energy/pressure loss. The low and high WSS values have also influenced the type of aneurysm growth, with high WSS promoting a small and thin wall aneurysm and low WSS promoting a large and thick wall aneurysm [10]. The simulation was limited to a saccular type aneurysm in the middle cerebral artery. Bazilevs *et al.*, [11] reported that saccular type aneurysms had high wall tension in the aneurysm dome, which indicated the location of the aneurysm. They discovered that when the wall tension is greater than the tissue strength, the aneurysm is more likely to rupture. Torii *et al.*, [12] conducted simulation studies on saccular type cerebral aneurysms with various hemodynamic conditions, focusing primarily on hypertension, which is claimed to be a major contributor to aneurysm growth and arterial tissue damage [12,13].

Fusiform aneurysms are found to occur at a 10% rate in the proximal and distal MCA. These aneurysms, like other aneurysms, can cause haemorrhages if they rupture and have other health implications if they affect nearby brain tissue and nerves. The causes and progression of this type of aneurysm are still being debated. Most researchers included the hemodynamic effect in their simulation, with the majority focusing on saccular type aneurysms. However, instead of solely focusing on the saccular type aneurysm and hemodynamic effect, the body temperature and fusiform type aneurysm must also be considered when evaluating factors that contribute to growth.

An aneurysm is a dilated or ballooned section of a blood vessel that appears in various locations throughout the cardiovascular system because of excess pressure or local weakness of the arterial wall [14-17,18]. When an aneurysm ruptures in the cerebral arteries, it causes subarachnoid haemorrhage (SAH), a type of stroke that can result in death or permanent disability. Previous research indicates that approximately 5% of the world's population develops an aneurysm, with only a fraction of these bursts [14,15]. In some cases, the aneurysm does not rupture but causes serious health problems such as vomiting, nerve paralysis, and headache because of compression of surrounding brain tissue and nerves [15]. Hemodynamic conditions can influence the growth and rupture of an intracranial aneurysm [19,20]. The factor influencing aneurysm growth at this stage still requires extensive research to fully understand the process [17,21-23]. There are two theories about the rupture of an aneurysm [24]. One of the theories agreed that the aneurysm rupture was caused by high WSS in the aneurysm wall. Other theories contend that a low WSS is associated with aneurysm rupture. The geometry of an aneurysm is determined by the WSS and the flow within the aneurysm [25]. The WSS is primarily determined by the mechanical properties of the arterial wall, aneurysm geometry, and aneurysm pressure [21,26-27]. Hypertension's systemic enhancement of the hemodynamic effect resulted in the formation, growth, and rupture of aneurysms [28,29].

Asymmetrical geometries of the anterior arteries have also been observed to contribute to the formation of cerebral artery aneurysms [28]. Although several surgical management for this type of aneurysm has been reported, the appropriate strategy or method remains unknown due to anatomical features and distal blood flow preservation [30]. Correct simulation techniques, such as computational fluid dynamic simulations, can aid medical expertise in preventing aneurysm rupture.

This paper discusses the relationship between body temperature and hemodynamic condition as it relates to wall shear stress at the arterial wall in the case of a fusiform cerebral aneurysm. Other researchers have not focused on the effect of hemodynamics and body temperature on the growth of fusiform type aneurysms in the current situation. Based on hemodynamic variables, three different models of fusiform aneurysms were identified, modelled, and simulated in this study. In this study, the computational fluid dynamics (CFD) analysis method is used to investigate the hemodynamic variable effect on the WSS on the aneurysmal wall. The simulations were carried out in a transient state with two cardiac cycles of abdominal blood pressure (ABP) and middle cerebral artery (MCA) velocity. The grid-independent test was carried out to ensure that the simulation results were accurate. The data was then analyzed and presented in terms of WSS and OSI index. According to the findings, the hypertension effect causes a significant change in the WSS distribution in the aneurysm wall, which may affect the aneurysm wall's growth and damage.

## **2. Methodology**

### *2.1 Geometry of Difference Aneurysm at The Cerebral Artery*

Magnetic resonance imaging was used to generate a three-dimensional model of the fusiform aneurysm based on the patient-specified model (MRI). The model was then remodelled in SolidWorks 2018 (Dassault Systèmes, United States, 2018), as shown in Figure 1. The first model of a middle fusiform aneurysm is depicted in Figure 1(a) [31]. This model has a symmetrical bulge diameter of 4 mm and a total length of 50.39 mm. The bulging volume depth is 4.7 mm, the bulge's maximum diameter is 6.06 mm, and the bulge area is 74 mm<sup>2</sup>. Furthermore, because the depth of the aneurysm is smaller than its diameter, this model remains in the fusiform category [32].

Figure 1(b) depicts the development of a second model of a posterior fusiform aneurysm [33]. This model was created in the context of a non-symmetrical fusiform aneurysm. The volume of the bulge, however, was not symmetrical to the aneurysm axis. The inlet diameter is 3 mm, and the overall length is 62 mm. The bulge area has a length of 15.5 mm, a maximum diameter of 8.5 mm, and a total bulge area of 319.25 mm<sup>2</sup>. The overall area of the model is approximately 858.41 mm<sup>2</sup>.

The posterior fusiform aneurysm was the third model, as shown in Figure 1(c) [34]. In this model, a non-symmetrical aneurysm with an inlet diameter of 4 mm and a total length of 57 mm was created. The bulge has a diameter of 10 mm and an area of 482.19 mm<sup>2</sup>. The model's total area is approximately 1282.55 mm<sup>2</sup>.

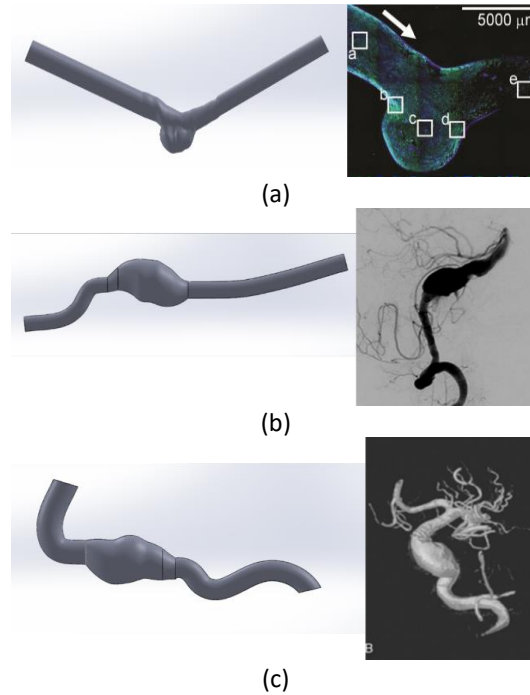


**Fig. 1.** Three different model of aneurysm (a) middle fusiform aneurysm [31] (b) anterior fusiform aneurysm [33] (c) posterior fusiform aneurysm [34]

## 2.2 Governing Equation

ANSYS Fluent 19.2 (ANSYS, Inc., United States, 2018) was used as the simulation and CFD analysis platform in this study. To solve the continuity, Navier-Stokes, and Energy equations, both velocity inlet and pressure outlet are computed. The conservation of mass and momentum are appropriate physical laws to represent when describing MCA problems. The continuity, Navier–Stokes, and energy equations for such a fluid are as follows [35,36-38].

$$\nabla \cdot \mathbf{u} = 0 \quad (1)$$

$$\rho \left( \frac{\partial \mathbf{u}}{\partial t} + \mathbf{u} \cdot \nabla \cdot \mathbf{u} \right) = -\nabla p + \mu \nabla \cdot \mathbf{u} \quad (2)$$

$$\frac{\partial(\rho e)}{\partial t} + \nabla \cdot (\rho \mathbf{u} e) = -\nabla \cdot (K \nabla T) + Se \quad (3)$$

where  $\mathbf{u}$  = velocity,  $P$  = Pressure,  $\rho$  = Density,  $e$  is the internal energy,  $Se$  is the source,  $K$  is the temperature gradient coefficient,  $T$  is the temperature, and  $\mu$  = Viscosity. The shear stress, WSS at the wall of the aneurysm is calculated based on a function of velocity gradient [23]. Where  $\frac{\partial \mathbf{u}}{\partial y}$  is the velocity gradient along the aneurismal wall taking fluid viscosity into account, and  $y$  is the distance from the wall.

$$WSS = \mu \left( \frac{\partial \mathbf{u}}{\partial y} \right)_{y=0} \quad (4)$$

The oscillatory shear index (OSI), a dimensionless parameter ranging from 0 to 0.5 that computes the magnitude of wall shear stress fluctuations, quantifies directional changes in wall shear stresses. The oscillatory shear index [23] at the aneurysm wall is computed as follows

$$OSI = \frac{1}{2} \left( 1 - \frac{\left| \int_0^T \overline{WSS}_i dt \right|}{\int_0^T |\overline{WSS}_i| dt} \right) \quad (5)$$

where  $t$  denotes time,  $WSS_i$  denotes the instantaneous WSS vector, and  $T$  denotes the cycle duration.

### 2.2.1 Discretization technique

The finite volume method is used to solve the governing equations on a spatially tetrahedral computational mesh designed in the Cartesian coordinate system and refined locally at the fluid's most outer volume surface. During the calculation, specific blood regions were refined further at the arterial and aneurysm surfaces. The mesh cell centres store all physical variables. To discretize the governing equations in a conservative form, the Finite Volume method is used. Figure 2 depicts the mesh of the aneurysmal model.

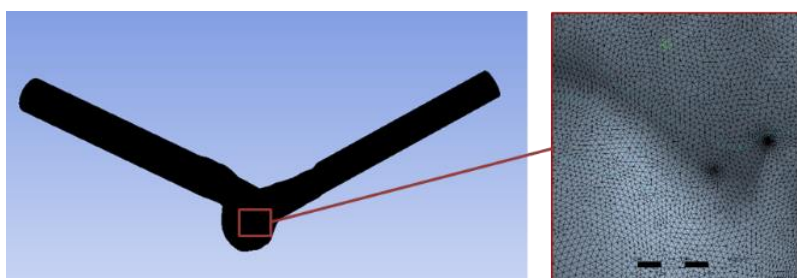


**Fig. 2.** Mesh generated in the middle fusiform aneurysm for the Model 1

### 2.3 Parameter and Boundary Conditions

Several assumptions were imposed on the developed model in this study, which include transient, incompressible flow, homogeneous, non-Newtonian flow for a shear rate less than  $100 \text{ s}^{-1}$ , and the flow were predicted as a pulsatile flow with a Reynolds number less than 200 [37,39]. Body temperatures ranging from normal to high were also included in the analyses to see how they affected the properties studied. Furthermore, two types of blood pressure flow were included in the study: normal and second-stage hypertension, to see how they affected blood flow in aneurysms. Fully developed parabolic flow with zero radial velocity at the inlet, no-slip at the wall, and zero velocity gradient at the outlet are the boundary conditions. For time-dependent operation, the inlet was also set to pulsatile velocity, while the outlet was set to pulsatile pressure.

The parameters and boundary conditions were set to be the same for the three models studied, with the assumption that the conditions are transient. Since the effect of temperature distributions was included in this study, the energy equation is used in the analyses. The SST k- $\omega$  turbulence model was used to calculate shear stress on the aneurysm wall. The blood properties used in the simulation are based on previous data from another researcher, which is summarised in Table 1 [40].

**Table 1**  
Blood properties used in the simulations

Properties	Value used
Density	1060 kg/m <sup>3</sup>
Specific heat	3.475 kJ/kg.K
Thermal conductivity	0.67 W/m.K
Viscosity	0.0035 kg/ms

### 3. Simulation results

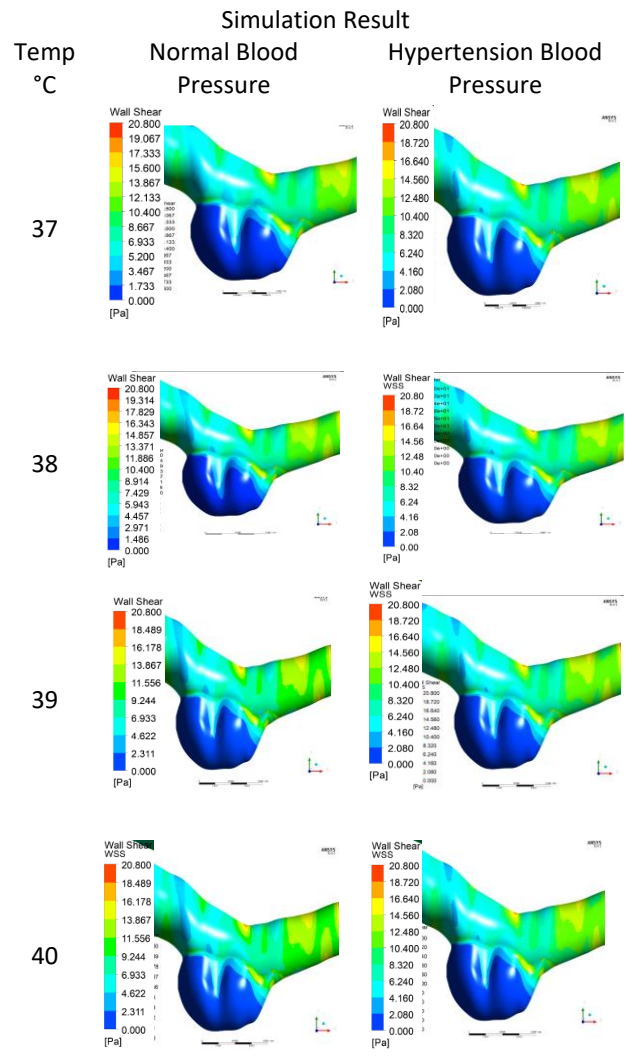
#### 3.1 Wall Shear Stress (WSS) and Oscillatory Shear Index (OSI) for Middle Fusiform Aneurysm

Figure 3 shows the distribution of WSS at the fusiform aneurysm in different temperatures with normal blood pressure (NBP) and high blood pressure (HBP) conditions. There were no significant changes in low WSS observed for the temperatures of 37°C and 38°C. However, at temperatures between 39°C and 40°C, there was a significant change in the low WSS area. The percentage area of WSS at 39°C was widened, particularly in the region of the aneurysm's neck. Similarly, the WSS distribution at the hotspot jet area remains constant across all temperature ranges. However, the distribution of low WSS in the hypertension condition resembles that of normal blood pressure for temperature differences. Low WSS in aneurysms could be caused by flow stagnation or vortices dominated at the bulge area [41,42].

Figure 4 shows the mean WSS in normal blood pressure for temperature differences for the first model of the aneurysm. From the observation, the highest mean WSS has indicated approximately at 3.761274 Pa for a body temperature of 38 °C. Then, the WSS slightly dropped after reaching the peak value and the lowest value of WSS is indicated at a temperature of 40 °C with the pressure approximately at 3.755481 Pa.

In hypertension conditions, the distribution of the mean WSS for different temperatures was slightly different, as shown in Figure 5. The mean WSS decreased slightly from 37°C to 39°C; however, the value of WSS increased slightly at 40°C. According to the observations, the highest mean WSS value was at 40 °C and the lowest at 39 °C, contributing approximately 5.705490 Pa and 5.075948 Pa, respectively.

OSI analysis is critical for determining the initial lesion and how far it has progressed in the aneurysm region. The lowest OSI value may be more likely to reduce the risk of aneurysmal wall rupture. As a result, Figure 6 presents the analysis of the OSI for various temperatures in both NBP and HBP. According to the observations, NBP has the highest OSI value when compared to HBP at various temperatures. However, the value of OSI was similar for both NBP and HBP at each temperature. The OSI index for NBP was found to be higher than that of HBP, with a 12.28 percent difference. Furthermore, the difference in the OSI at different temperatures was calculated for both NBP and HBP, which contributed approximately 0.002 percent and 0.311 percent, respectively. The difference in OSI values for NBP and HBP has a significant effect on the distribution of low WSS, with low WSS producing higher OSI [43].



**Fig. 3.** Distributions of Normal Blood Pressure and Hypertension condition with different temperatures for Model 1

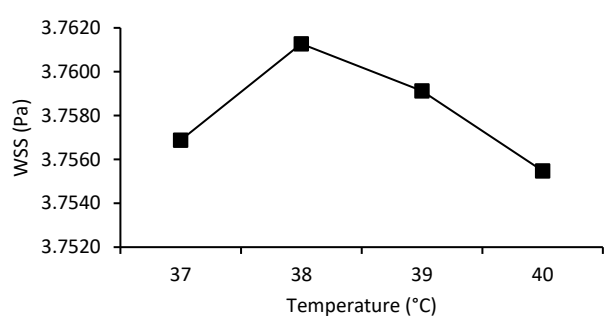


**Fig. 4.** Distribution of mean WSS in normal blood pressure for the first model aneurysm

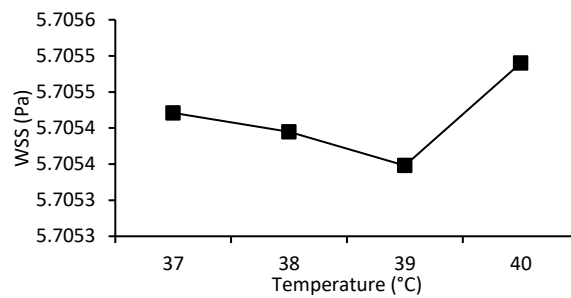


**Fig. 5.** The mean WSS in hypertension for the first model for different temperatures

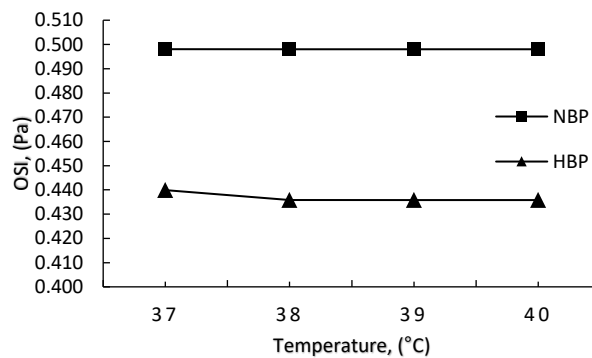


**Fig. 6.** Oscillatory Shear Index for both NBP and hypertension for the first model of aneurysm

### 3.2 Wall Shear Stress (WSS) and Oscillatory Shear Index (OSI) for Anterior Fusiform Aneurysm

WSS distribution has a significant impact on the geometry of aneurysms. The saccular aneurysm demonstrated flow fluctuation in the aneurysmal region, which promotes high WSS. However, the effect of WSS in the anterior aneurysm is explained differently, as shown in Figure 7. This graph represents the distribution of WSS at anterior aneurysms for both NBP and HBP at different temperatures. WSS distributions were found to be highest at the proximal neck of the anterior aneurysm compared to the distal region. The highest WSS value was at the aneurysm bulge and the lowest was 0.00296 Pa for the HBP condition. Otherwise, the NBP condition yielded the lowest WSS value of around 0.00578 Pa. This is an indication of an increase in the rate of aneurysm growth during hypertension blood pressure conditions [44]. The lowest region of the WSS was more likely to promote thrombosis and increase pressure distribution at the anterior aneurysm. Temperature changes, on the other hand, have a minor impact on low WSS areas.

Figure 8 and 9 show the detailed effects of WSS at various temperatures on the anterior fusiform aneurysm. According to the findings, the lowest WSS value was observed at 38°C for both NBP and HBP conditions, which are approximately 3.3698820 Pa and 5.421 Pa, respectively. However, the highest WSS values were observed at 37°C for NBP and 40°C for HBP conditions, which contributed approximately 3.708485 Pa and 5.425 Pa, respectively. In comparison, the WSS value at HBP was found to be higher than at NBP. As a result of the HBP condition, the WSS distribution has a significant effect. WSS values recorded at 39 °C and 40 °C in NBP conditions do not change as the temperature rises.

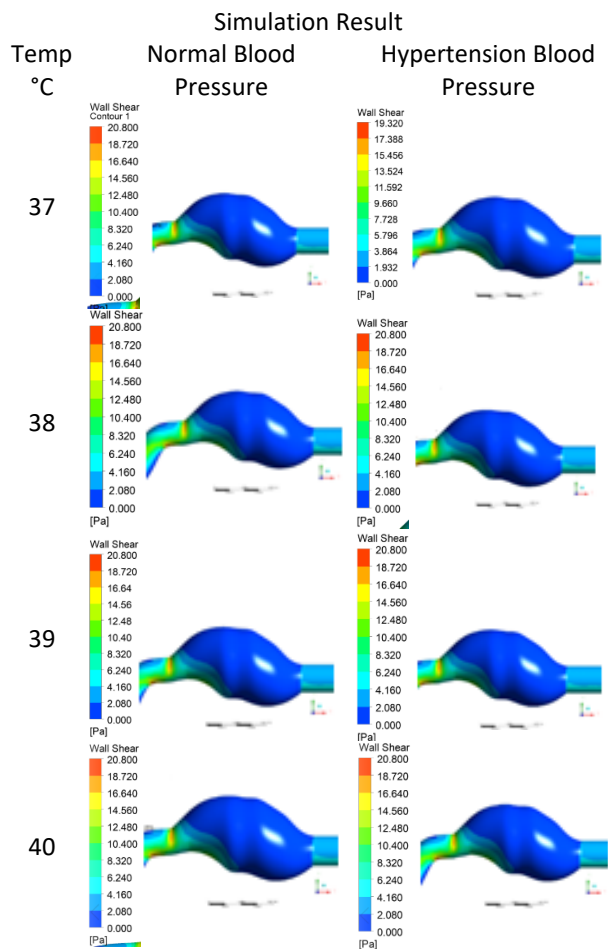


**Fig. 7.** Distribution of WSS for both NBP and HBP in different temperatures for the second model of aneurysm

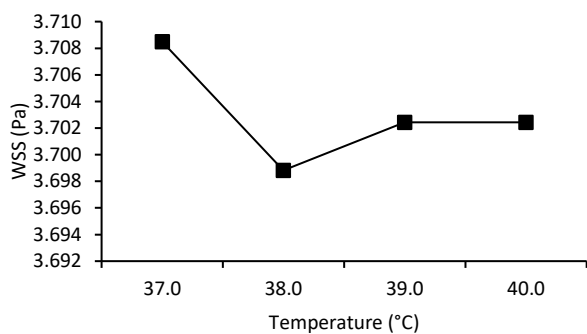


**Fig. 8.** The mean WSS for NBP for different temperatures

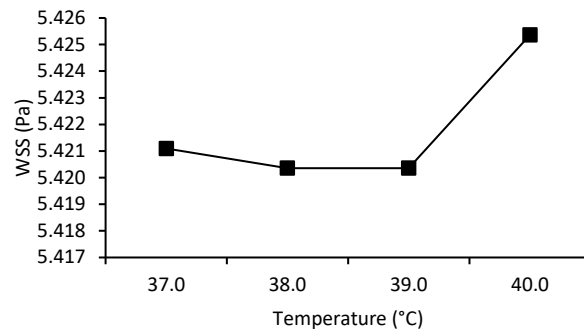


**Fig. 9.** The mean WSS at the hypertension condition the anterior fusiform aneurysm

The fluctuation of flow has a significant impact on the aneurismal wall failure. The OSI index may be useful in predicting the failure of the aneurismal wall by predicting the strength of the vortices. A lower OSI index value may indicate a lower risk of aneurismal failure. Figure 10 represents the OSI analysis for both NBP and HBP at various temperatures for the model under consideration. The OSI index discrepancy for both NBP and HBP was approximately 8.86 percent. Both physiological conditions at different temperatures showed a similar pattern of OSI value. However, the highest OSI was observed in the NBP condition rather than the HBP condition, which contributed about 0.48 and 0.435, respectively.

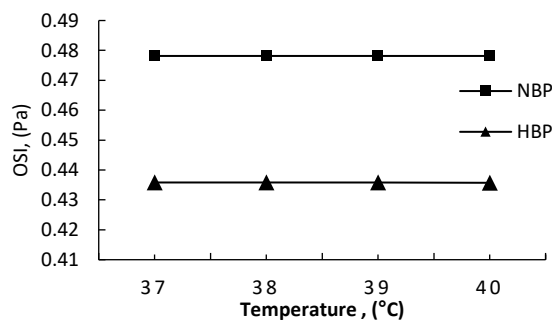


**Fig 10.** Oscillatory Shear Index for both blood pressure in model

### 3.3 Wall Shear Stress (WSS) and Oscillatory Shear Index (OSI) for Posterior Fusiform Aneurysm

WSS has a significant effect on the different geometries of the aneurysm. This phenomenon occurred as a result of the different flow characteristics displayed in the various geometries. The deformation of arteries as temperature rises contributes to the variation trend of WSS in NBP and HBP conditions [45].

The geometry of the vessel, which represents the presence of various failure risks, also affected the flow direction alignment. The WSS and OSI analyses in posterior fusiform aneurysms were explained in this section. Figure 11 shows the distribution of WSS at various temperatures for both NBP and HBP in the case of a posterior fusiform aneurysm. Flow recirculation was seen at the distal neck as opposed to the proximal neck based on the observations. The distal region of the posterior fusiform aneurysm had the highest WSS, predicting the weakest region of the artery. The pattern of WSS distribution, on the other hand, was quite similar for both NBP and HBP conditions.

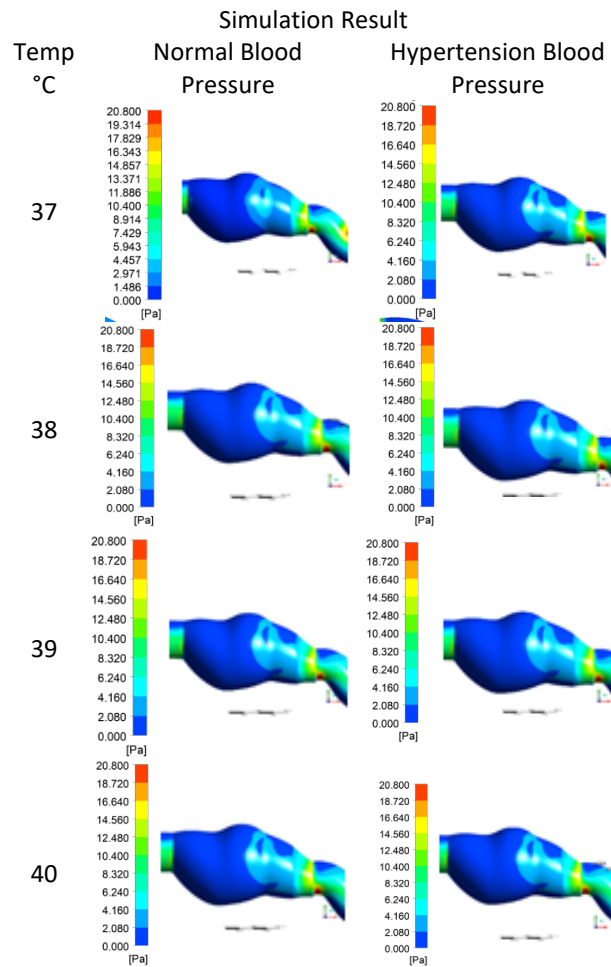


**Fig. 11.** Distributions of WSS for both NBP and HBP conditions for various temperature differences at the posterior fusiform aneurysm

For both NBP and HBP conditions, the low WSS dominated the overall area of the posterior fusiform aneurysm. As shown in Figure 12 and 13, the mean WSS was calculated for both NBP and HBP conditions. The HBP condition had the highest mean WSS, with a discrepancy of about 25%. However, the mean WSS in NBP increases from 37°C to 38°C, then remains constant until the temperature reaches 40°C. The HBP condition, on the other hand, had a different mean WSS behaviour throughout the temperature difference. The mean WSS in HBP decreased slightly between temperatures of 37°C and 38°C and remained constant at temperatures of 38°C, 39°C, and 40°C.

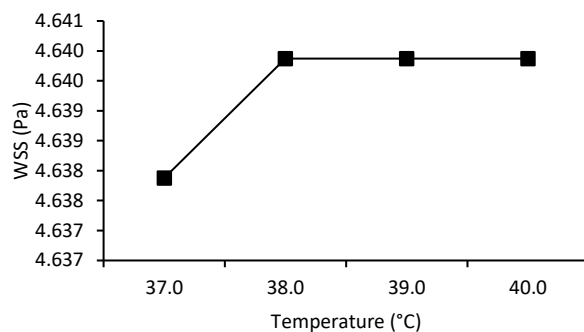


**Fig. 12.** The mean WSS for NBP condition in different temperatures for the posterior fusiform aneurysm region

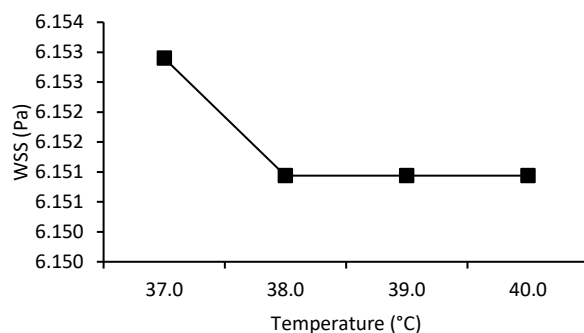


**Fig. 13.** The mean WSS for HBP conditions in different temperatures different

Figure 14 represents the OSI index for both NBP and HBP conditions at different temperatures at a posterior fusiform aneurysm. The pattern of OSI for all geometries was observed to be similar for both NBP and HBP. For all models, the OSI index was highest in the NBP condition. Furthermore, the OSI index value has remained consistent across temperature differences for both NBP and HBP conditions.

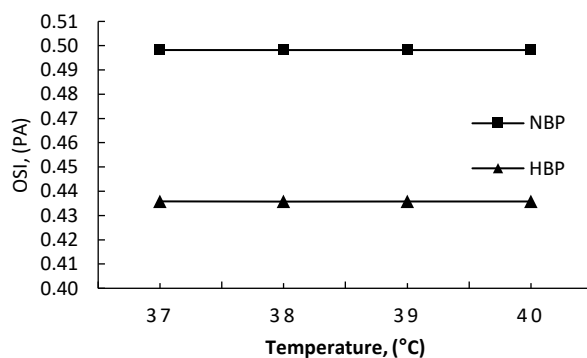


**Fig. 14.** Oscillatory Shear Index for both blood pressure conditions in model 3

## 5. Conclusions

The various geometries of fusiform aneurysms represent different hemodynamic effects on the aneurismal wall under different physiological conditions. According to the findings, the anterior fusiform aneurysm had the lowest WSS and OSI value when compared to other geometries. Furthermore, flow recirculation was seen at the aneurysm's distal neck for the middle and posterior aneurysms, but not at the proximal neck for the anterior fusiform aneurysm. WSS values fluctuated in different temperatures for both physiological conditions at all geometries of the aneurysm. The OSI value, on the other hand, yielded similar results in different temperatures for each physiological condition. In hypertension (HBP) conditions, the higher the temperature, the higher the WSS, which may predict the weakest point of the aneurysm to rupture.

## Acknowledgement

This research was funded by a grant from Universiti Tun Hussein Onn Malaysia (Tier 1 Grant H818).

## References

- [1] Kinoshita, Masashi, Shinya Kida, Mitsuhiro Hasegawa, Junkoh Yamashita, and Motohiro Nomura. "Pathological examination of a ruptured fusiform aneurysm of the middle cerebral artery." *Surgical Neurology International* 5, no. Suppl 12 (2014): S465. <https://doi.org/10.4103/2152-7806.143722>
- [2] Serulle, Yafell, Deepak Khatri, Jada Fletcher, Anna Pappas, Audrey Heidebreder, David Langer, and Rafael A. Ortiz. "Fusiform superior cerebellar artery aneurysm treated with flow diversion: A case report." *Surgical Neurology International* 11 (2020). [https://doi.org/10.25259/SNI\\_556\\_2020](https://doi.org/10.25259/SNI_556_2020)
- [3] Griffin, Andrew, Emily Lerner, Adam Zuchowski, Ali Zomorodi, L. Fernando Gonzalez, and Erik F. Hauck. "Flow diversion of fusiform intracranial aneurysms." *Neurosurgical Review* 44, no. 3 (2021): 1471-1478. <https://doi.org/10.1007/s10143-020-01332-0>
- [4] Dzhindzhikhadze, Revaz, Andrey Polyakov, Oleg Dreval, and Valeriy Lazarev. "Successful microsurgical clipping of ruptured fusiform aneurysm of the anterior cerebral artery. Case report and review of the literature." *Surgical Neurology International* 11 (2020). [https://doi.org/10.25259/SNI\\_727\\_2020](https://doi.org/10.25259/SNI_727_2020)
- [5] Li, Miao, Jie Wang, Jian Liu, Conghai Zhao, and Xinjian Yang. "Hemodynamics in ruptured intracranial aneurysms with known rupture points." *World neurosurgery* 118 (2018): e721-e726. <https://doi.org/10.1016/j.wneu.2018.07.026>
- [6] Jiang, Pengjun, Qingyuan Liu, Jun Wu, Xin Chen, Maogui Li, Zhengsong Li, Shuzhe Yang et al. "Hemodynamic characteristics associated with thinner regions of intracranial aneurysm wall." *Journal of Clinical Neuroscience* 67 (2019): 185-190. <https://doi.org/10.1016/j.jocn.2019.06.024>
- [7] Jiang, Jingfeng, and Charles Strother. "Computational fluid dynamics simulations of intracranial aneurysms at varying heart rates: a "patient-specific" study." *Journal of biomechanical engineering* 131, no. 9 (2009). <https://doi.org/10.1115/1.3127251>
- [8] Isaksen, Jørgen Gjernes, Yuri Bazilevs, Trond Kvamsdal, Yongjie Zhang, Jon H. Kaspersen, Knut Waterloo, Bertil Romner, and Tor Ingebrigtsen. "Determination of wall tension in cerebral artery aneurysms by numerical simulation." *Stroke* 39, no. 12 (2008): 3172-3178. <https://doi.org/10.1161/STROKEAHA.107.503698>
- [9] Xu, Lijian, Lixu Gu, and Hao Liu. "Exploring potential association between flow instability and rupture in patients with matched-pairs of ruptured–unruptured intracranial aneurysms." *Biomedical engineering online* 15, no. 2 (2016): 461-477. <https://doi.org/10.1186/s12938-016-0277-8>
- [10] Meng, H., V. M. Tutino, J. Xiang, and A. Siddiqui. "High WSS or low WSS? Complex interactions of hemodynamics with intracranial aneurysm initiation, growth, and rupture: toward a unifying hypothesis." *American Journal of Neuroradiology* 35, no. 7 (2014): 1254-1262. <https://doi.org/10.3174/ajnr.A3558>
- [11] Bazilevs, Y., M-C. Hsu, Y. Zhang, W. Wang, T. Kvamsdal, S. Hentschel, and J. G. Isaksen. "Computational vascular fluid–structure interaction: methodology and application to cerebral aneurysms." *Biomechanics and modeling in mechanobiology* 9, no. 4 (2010): 481-498. <https://doi.org/10.1007/s10237-010-0189-7>
- [12] Torii, Ryo, Marie Oshima, Toshio Kobayashi, Kiyoshi Takagi, and Tayfun E. Tezduyar. "Fluid–structure interaction modeling of aneurysmal conditions with high and normal blood pressures." *Computational Mechanics* 38, no. 4 (2006): 482-490. <https://doi.org/10.1007/s00466-006-0065-6>

- [13] Sforza, Daniel M., Christopher M. Putman, and Juan R. Cebal. "Computational fluid dynamics in brain aneurysms." *International journal for numerical methods in biomedical engineering* 28, no. 6-7 (2012): 801-808. <https://doi.org/10.1002/cnm.1481>
- [14] Ugron, Ádám, and György Paál. "On the boundary conditions of cerebral aneurysm simulations." *Periodica Polytechnica Mechanical Engineering* 58, no. 1 (2014): 37-45. <https://doi.org/10.3311/PPme.7392>
- [15] Fukuda, Shunichi, Yuji Shimogonya, Masanori Nakamura, Tomohiro Yamada, Kosuke Suzuki, Yuuto Yamamoto, Kiyomitsu Kanou et al. "Review on the formation and growth of cerebral aneurysms." *Journal of Biomechanics* 33, no. 2 (2019): 43-52. <https://doi.org/10.17106/jbr.33.43>
- [16] Algabri, Yousif A., Surapong Chatpun, and Ishkrizat Taib. "An investigation of pulsatile blood flow in an angulated neck of abdominal aortic aneurysm using computational fluid dynamics." *Journal of Advanced Research in Fluid Mechanics and Thermal Sciences* 57, no. 2 (2019): 265-274.
- [17] Dabagh, Mahsa, Priya Nair, John Gounley, David Frakes, L. Fernando Gonzalez, and Amanda Randles. "Hemodynamic and morphological characteristics of a growing cerebral aneurysm." *Neurosurgical focus* 47, no. 1 (2019): E13. <https://doi.org/10.3171/2019.4.FOCUS19195>
- [18] Shafii, Nadia Shaira, Ryuhei Yamaguchi, Ahmad Zahran Md Khudzari, Gaku Tanaka, Atsushi Saitoh, Makoto Ohta, and Kahar Osman. "Hemodynamic and Flow Recirculation Effect on Rupture Prediction of Middle Cerebral Artery Aneurysm." *Journal of Advanced Research in Fluid Mechanics and Thermal Sciences* 79, no. 1 (2020): 1-16. <https://doi.org/10.37934/arfmts.79.1.116>
- [19] Kaspera, Wojciech, Piotr Ładziński, Patrycja Larysz, Anna Hebda, Krzysztof Ptaszekiewicz, Marek Kopera, and Dawid Larysz. "Morphological, hemodynamic, and clinical independent risk factors for anterior communicating artery aneurysms." *Stroke* 45, no. 10 (2014): 2906-2911. <https://doi.org/10.1161/STROKEAHA.114.006055>
- [20] Khairi, Nur Afikah, Mohd Azrul Hisham Mohd Adib, Nur Hazreen Mohd Hasni, and Mohd Shafie Abdullah. "Effect of Hemodynamic Parameters on Physiological Blood Flow through Cardiovascular Disease (CVD)—The Perspective Review." *Journal of Advanced Research in Fluid Mechanics and Thermal Sciences* 74, no. 1 (2020): 19-34. <https://doi.org/10.37934/arfmts.74.1.1934>
- [21] Omodaka, Shunsuke, Shin-ichirou Sugiyama, Takashi Inoue, Kenichi Funamoto, Miki Fujimura, Hiroaki Shimizu, Toshiyuki Hayase, Akira Takahashi, and Teiji Tominaga. "Local hemodynamics at the rupture point of cerebral aneurysms determined by computational fluid dynamics analysis." *Cerebrovascular Diseases* 34, no. 2 (2012): 121-129. <https://doi.org/10.1159/000339678>
- [22] Zhang, Yisen, Zhongbin Tian, Linkai Jing, Ying Zhang, Jian Liu, and Xinjian Yang. "Bifurcation type and larger low shear area are associated with rupture status of very small intracranial aneurysms." *Frontiers in Neurology* 7 (2016): 169. <https://doi.org/10.3389/fneur.2016.00169>
- [23] Murayama, Yuichi, Soichiro Fujimura, Tomoaki Suzuki, and Hiroyuki Takao. "Computational fluid dynamics as a risk assessment tool for aneurysm rupture." *Neurosurgical focus* 47, no. 1 (2019): E12. <https://doi.org/10.3171/2019.4.FOCUS19189>
- [24] Miura, Yoichi, Fujimaro Ishida, Yasuyuki Umeda, Hiroshi Tanemura, Hidenori Suzuki, Satoshi Matsushima, Shinichi Shimosaka, and Waro Taki. "Low wall shear stress is independently associated with the rupture status of middle cerebral artery aneurysms." *Stroke* 44, no. 2 (2013): 519-521. <https://doi.org/10.1161/STROKEAHA.112.675306>
- [25] Wang, Fuyu, Bainan Xu, Zhenghui Sun, Chen Wu, and Xiaojun Zhang. "Wall shear stress in intracranial aneurysms and adjacent arteries." *Neural regeneration research* 8, no. 11 (2013): 1007. <https://doi.org/10.3969/j.issn.1673-5374.2013.11.006>
- [26] Shishir, Shamiul Sarkar, Md Abdul Karim Miah, AKM Sadrul Islam, and ABM Toufique Hasan. "Blood flow dynamics in cerebral aneurysm—A CFD simulation." *Procedia Engineering* 105 (2015): 919-927. <https://doi.org/10.1016/j.proeng.2015.05.116>
- [27] Razhali, Nur Farahalya, and Ishkrizat Taib. "Analysis of Hemodynamic on Different Stent Strut Configurations in Femoral Popliteal Artery." *CFD Letters* 14, no. 3 (2022): 119-128. <https://doi.org/10.37934/cfdl.14.3.119128>
- [28] Vlak, Monique HM, Gabriel JE Rinkel, Paut Greebe, and Ale Algra. "Risk of rupture of an intracranial aneurysm based on patient characteristics: a case-control study." *Stroke* 44, no. 5 (2013): 1256-1259. <https://doi.org/10.1161/STROKEAHA.111.000679>
- [29] Hong, Lim Sheh, Mohd Azrul Hisham Mohd Adib, Mohd Shafie Abdullah, and Radhiana Hassan. "Qualitative and Quantitative Comparison of Hemodynamics Between MRI Measurement and CFD Simulation on Patientspecific Cerebral Aneurysm—A Review." *Journal of Advanced Research in Fluid Mechanics and Thermal Sciences* 68, no. 2 (2020): 112-123. <https://doi.org/10.37934/arfmts.68.2.112123>
- [30] Aoki, Yoshinori, Masaaki Nemoto, Kyosuke Yokota, Toshiyuki Kano, Shouzou Goto, and Nobuo Sugo. "Ruptured Fusiform Aneurysm of the Proximal Anterior Cerebral Artery (A1 Segment)—Case Report—." *Neurologia medico-chirurgica* 47, no. 8 (2007): 351-355. <https://doi.org/10.2176/nmc.47.351>

- [31] Levitt, Michael R., Christian Mandrycky, Ashley Abel, Cory M. Kelly, Samuel Levy, Venkat K. Chivukula, Ying Zheng, Alberto Aliseda, and Louis J. Kim. "Genetic correlates of wall shear stress in a patient-specific 3D-printed cerebral aneurysm model." *Journal of neurointerventional surgery* 11, no. 10 (2019): 999-1003. <https://doi.org/10.1136/neurintsurg-2018-014669>
- [32] Larrabide, I., M. L. Aguilar, H. G. Morales, A. J. Geers, Z. Kulcsár, D. Rüfenacht, and A. F. Frangi. "Intra-aneurysmal pressure and flow changes induced by flow diverters: relation to aneurysm size and shape." *American Journal of Neuroradiology* 34, no. 4 (2013): 816-822. <https://doi.org/10.3174/ajnr.A3288>
- [33] Kizilkilic, Osman, Yasemin Kayadibi, Galip Zihni Sanus, Naci Koçer, and Civan Islak. "Combined endovascular and surgical treatment of fusiform aneurysms of the basilar artery." *Acta neurochirurgica* 156, no. 1 (2014): 53-61. <https://doi.org/10.1007/s00701-013-1913-8>
- [34] "Vascular Anomalies of the Brain." Radiology Key (2016).
- [35] Sousa, Luisa Costa, Catarina F. Castro, and Carlos Conceição António. "Blood flow simulation and applications." In *Technologies for medical sciences*, pp. 67-86. Springer, Dordrecht, 2012. [https://doi.org/10.1007/978-94-007-4068-6\\_4](https://doi.org/10.1007/978-94-007-4068-6_4)
- [36] Yusof, Nur Syamila, Siti Khuzaimah Soid, Mohd Rijal Ilias, Ahmad Sukri Abd Aziz, and Nor Ain Azeany Mohd Nasir. "Radiative Boundary Layer Flow of Casson Fluid Over an Exponentially Permeable Slippery Riga Plate with Viscous Dissipation." *Journal of Advanced Research in Applied Sciences and Engineering Technology* 21, no. 1 (2020): 41-51. <https://doi.org/10.37934/araset.21.1.4151>
- [37] Jamali, Muhammad Sabaruddin Ahmad, and Zuhaila Ismail. "Simulation of Heat Transfer on blood flow through a stenosed bifurcated artery." *Journal of Advanced Research in Fluid Mechanics and Thermal Sciences* 60, no. 2 (2019): 310-323.
- [38] Alfarawi, Suliman SS, Azeldin El-sawi, and Hossin Omar. "Exploring Discontinuous Meshing for CFD Modelling of Counter Flow Heat Exchanger." *Journal of Advanced Research in Numerical Heat Transfer* 5, no. 1 (2021): 26-34.
- [39] Shafie, Sharidan, Rahimah Mahat, and Fatihhi Januddi. "Numerical Solutions of Mixed Convection Flow Past a Horizontal Circular Cylinder with Viscous Dissipation in Viscoelastic Nanofluid." *Journal of Advanced Research in Micro and Nano Engineering* 1, no. 1 (2020): 24-37.
- [40] Sherif, Camillo, Erwin Herbich, Roberto Plasenzotti, Helga Bergmeister, Ursula Windberger, Georg Mach, Gerhard Sommer et al. "Very large and giant microsurgical bifurcation aneurysms in rabbits: Proof of feasibility and comparability using computational fluid dynamics and biomechanical testing." *Journal of neuroscience methods* 268 (2016): 7-13. <https://doi.org/10.1016/j.jneumeth.2016.04.020>
- [41] Castro, Marcelo A. "Understanding the role of hemodynamics in the initiation, progression, rupture, and treatment outcome of cerebral aneurysm from medical image-based computational studies." *International Scholarly Research Notices* 2013 (2013). <https://doi.org/10.5402/2013/602707>
- [42] Castro, Marcelo A. "Understanding the role of hemodynamics in the initiation, progression, rupture, and treatment outcome of cerebral aneurysm from medical image-based computational studies." *International Scholarly Research Notices* 2013 (2013). <https://doi.org/10.5402/2013/602707>
- [43] Wan, Hailin, Liang Ge, Lei Huang, Yeqing Jiang, Xiaochang Leng, Xiaoyuan Feng, Jianping Xiang, and Xiaolong Zhang. "Sidewall aneurysm geometry as a predictor of rupture risk due to associated abnormal hemodynamics." *Frontiers in Neurology* 10 (2019): 841. <https://doi.org/10.3389/fneur.2019.00841>
- [44] Sheng, Bin, Degang Wu, Jinlong Yuan, Shanshui Xu, Zhenbao Li, Jin Dong, Niansheng Lai, and Xinggen Fang. "Hemodynamic characteristics associated with paraclinoid aneurysm recurrence in patients after embolization." *Frontiers in Neurology* 10 (2019): 429. <https://doi.org/10.3389/fneur.2019.00429>
- [45] Atienza, José M., Gustavo V. Guinea, Francisco J. Rojo, Raúl J. Burgos, Carlos García-Montero, Francisco J. Goicolea, Paloma Aragoncillo, and Manuel Elices. "Influencia de la presión y la temperatura en el comportamiento de la aorta y las carótidas humanas." *Revista española de cardiología* 60, no. 3 (2007): 259-267. <https://doi.org/10.1157/13100277>